Section 2
PROGRESS IN LASER FUSION

2.A Observation of Brillouin Sidescatter in Laser-Produced Plasma

We have recently obtained spectrally resolved measurements of scattered light from spherical targets at angles between 26° and 56° with respect to the laser axis. These experiments were designed to help distinguish between stimulated Brillouin scattering and reflection of refraction from the subcritical region. From these measurements we conclude that the sidescatter observed is attributable in most cases to Brillouin scattering.

Both theory and experiment have shown that appreciable Brillouin scattering will only occur for plasmas with long scalelengths. These long scalelengths are very likely to be important in future laser fusion experiments particularly those presently under consideration for UV, "blue," light. In order to produce these long scalelengths, we have used two different type pulses:
1. a 140 psec (FWHM) pulse following an intentional prepulse[20],
2. a 700 psec (FWHM) pulse, temporally Gaussian with no prepulse.

This experiment used one beam of the Glass Development Laser (GDL) at the Laboratory for Laser Energetics[21]. The 80 to 90 μm diameter glass microballoon targets were irradiated by circularly polarized laser light ($\lambda = 1.054\mu$m) at powers of up to 100 GW with pulse lengths of (A) 140 psec and (B) 700 psec. For

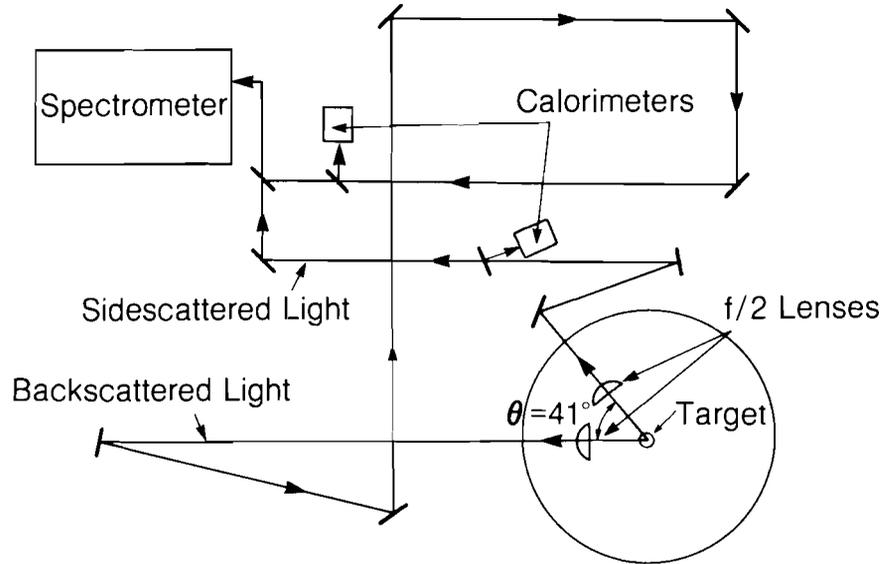Figure 22
Experimental layout for sidescattering at $\lambda_L = 1.06\mu m$.

most of the type (A) pulses, a prepulse with controlled magnitude and timing was inserted ahead of a main pulse to simulate an extensive underdense plasma region which would result from the use of a longer pulse. The prepulse energy was typically 1% of the main pulse energy, and the time between pulses was 1 nsec. An f/2 aspherical lens was used to focus the incident beam onto the target. The focal spot size was determined from x-ray pinhole photographs to be approximately 35 μm in diameter. The peak intensity was between 10^{15} and 10^{16} W/cm² in both cases. Figure 22 shows the experimental setup. The light which was directly backscattered through the focusing lens was reduced in size, collimated via an inverse telescope, and split into two beams for energy and spectral measurements. The sidescattered light was collected by an identical f/2 aspherical lens placed at 41° to the incident beam axis. This sidescatter beam was also analyzed for both energy and spectrum.

A 1 m Czerny-Turner grating spectrometer with 1 Å resolution was used for both back and sidescattered light spectra which were recorded on Kodak 4143 highspeed IR film.

An example of both back and sidescattered light spectra obtained with two different pulse shapes is shown in Figure 23. Figure 23a, which illustrates a type (A) pulse at laser intensity of 5 x 10^{15} W/cm² showed a red shift of the peak of ~3 Å for the backscatter and ~5 Å for the sidescatter from the ω_L incident laser frequency and a maximum shift 50 Å and 40 Å respectively. In separate experiments but with the same type (A) pulse, the hot electron temperature T_{HOT} and the typical density scalelength were measured to be 10 KeV[22] and 20 μm[23] respectively. The

Brillouin scattering threshold for an inhomogeneous plasma is given by[24]:

$$P_{SBS} > (1.6 \times 10^{14})\, T_e \text{ W/cm}^2,$$

where T_e (KeV) is the electron temperature driving an ion acoustic wave in an underdense plasma. Thus, since T_{HOT} is the upper limit for T_e, our laser intensity was well above the threshold, and the measured spectral red shifts were considered due to the stimulated Brillouin process. In the type (A) pulse we see no evidence for an unshifted (ω_L) spectral component in either the back or sidescattered light. The type (B) case of the 700 psec pulse at the intensity of 3.4×10^{15} W/cm² showed a somewhat different pattern. In addition to the red-shifted spectrum seen in both back and sidescattered light, the sidescattered spectrum contained a significant unshifted component in Figure 23b. This unshifted component is assumed to come from refracted incident light. Specular reflection may be ruled out as there is no comparable component in the direct backscatter. This clearly indicates the ability of this experiment to differentiate between the stimulated scattered component and the refracted or reflected light through angular resolved spectra. The finer angular distribution of the scattered light was measured using portions of the sidescatter collection lens. A mask with three apertures was used to give equal solid angle observations horizontally at $\Theta = 31°, 41°,$ and $51°$ with respect to the incident laser beam axis. The effective f number for each aperture was 6.7.
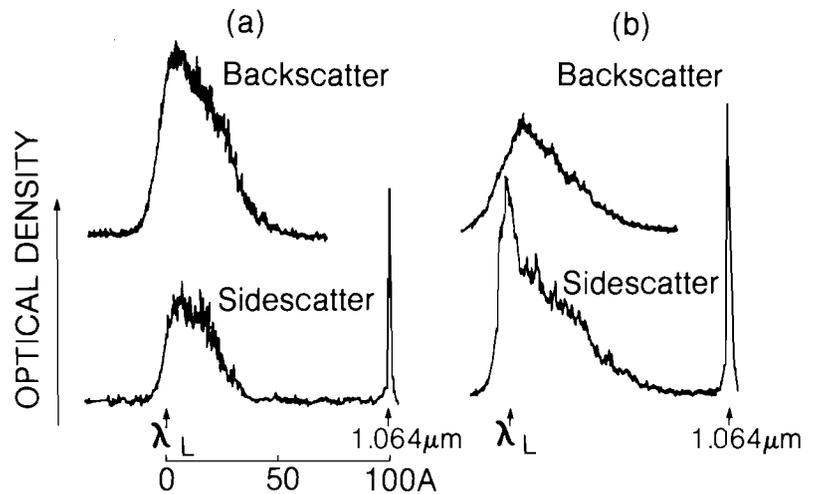
Figure 23

Back and sidescatter spectra for
a. type (A) pulse (prepulse +
140 psec pulse)
$I_L = 5 \times 10^{15}$ W/cm²
b. type (B) pulse (700 psec pulse)
$I_L = 3.4 \times 10^{15}$ W/cm²
OD is not in scale.

The measured angular energy distributions for two power levels are shown in Figure 24. In both experimental curves, the scattered light intensity falls rather rapidly as the angle increases. The decrease in intensity with scattering angle is somewhat more rapid than would be predicted by a one-dimensional model[25]. This result is not surprising since the plasma expansion geometry produced by illuminating 35 μm of a
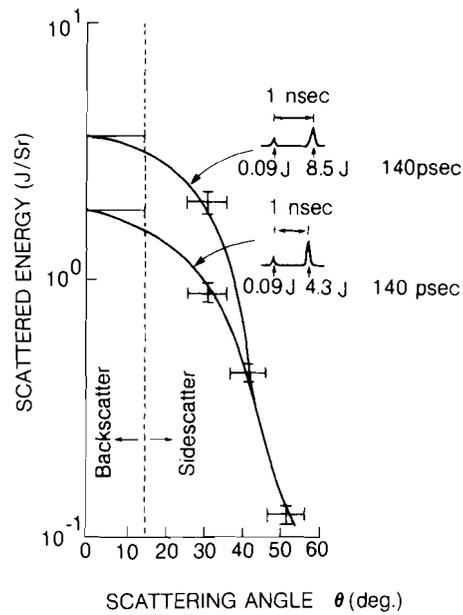
Figure 24

Angular distribution of stimulated Brillouin scatter for type (A) pulse. θ: angle with respect to incident laser axis.

80 μm diameter microballoon is unlikely to be represented by a one-dimensional planar expansion. The use of circular polarization for the incident beam allows one to assume axial symmetry for the scattered light. With this assumption of symmetry, the solid angle of the measured sidescatter light (S_1, 26° $\leq \Theta \leq$ 56°) was about 10 times larger than that of the backscattered light through the focusing lens (S_{FL}, 0° $\leq \Theta \leq$ 15°) as seen in Figure 25. Thus, although the energy scattered per unit solid angle (J/Sr) falls rather sharply with increasing angle (see Figure 24), the effective solid angle was large enough that the integrated energy in sidescattering was significant compared to
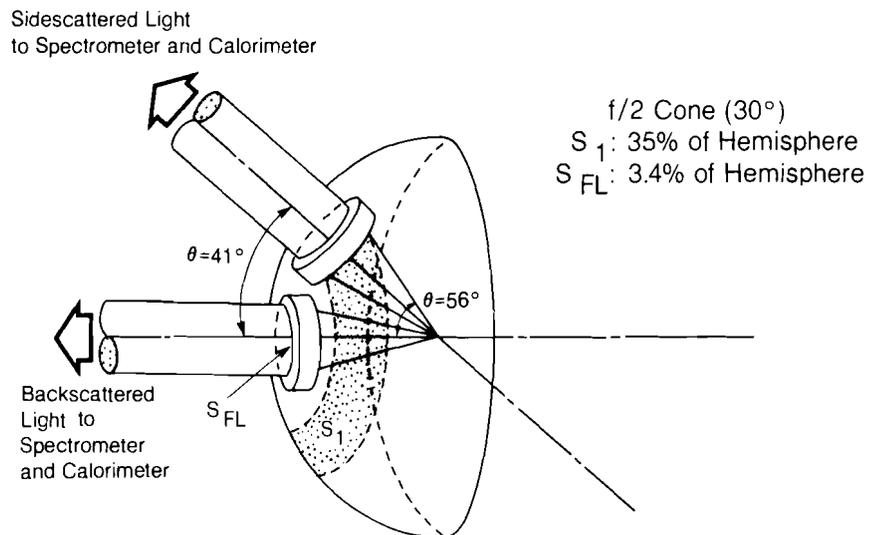

Figure 25

Sidescatter measurement configuration.